# Palm oil-based bio-PCM for energy efficient building applications: multipurpose thermal investigation and life cycle assessment

Claudia Fabiani[1], Anna Laura Pisello[1,2], Marco Barbanera[1,3], Luisa F. Cabeza [4]

[1] *CIRIAF - Interuniversity Research Center - University of Perugia. Via G. Duranti 63 06125, Perugia (Italy)*

[2] *Department of Engineering - University of Perugia. Via G. Duranti 97 06125, Perugia (Italy)*

[3] *Department of Economics, Engineering, Society and Business Organization - University of Tuscia. Via del paradiso 47 - 01100, Viterbo (Italy)*

[4] *GREiA Research Group, INSPIRES Research Centre - Universitat de Lleida. Pere de Cabrera s/n - 25001, Lleida (Spain)*

**Abstract**

This study aims at investigating the potential use of a bio-based phase change material, i.e. expired palm oil from the food industry, as a more sustainable alternative to petrochemical-based organic PCMs. To this purpose, thermogravimetric analysis (TGA) and isoconversional methods (Starink and Miura-Maki methods) are applied and the main thermo-physical properties of the blend are investigated by means of differential scanning calorimetry (DSC) and extensive thermal monitoring in a controlled realistic environment. Finally, a life cycle assessment is used to evaluate the environmental impact of the bio-based material in comparison to the more common petrochemical-based application. Kinetic analysis results indicate the two dimensional phase boundary reaction model as the most reliable scheme for describing the oxidation of palm oil, with an activation energy of about 73 $kJ \cdot mol^{-1}$. The DSC and the thermal monitoring procedure, showed two separate melting peaks in the ambient temperature range, which globally guarantee a melting enthalpy of about 50 $kJ \cdot kg^{-1}$, i.e. of the same order of magnitude of the first developed PCMs. Results from the life cycle analysis reveal that the expired palm oil can be considered a promising material for bio-based latent applications.

Globally, the palm oil has proved itself as a promising, low cost, and environmentally friendly alternative for passive thermal storage solutions (e.g. building envelope applications) where stability across multiple thermal cycles, low health risks, and low leakage are crucial parameters to be addressed.

*Keywords:* Phase change material, bio-based materials, industry-waste materials, DSC, TGA, energy efficiency

---

## 1. Introduction

Recent European policies have been tackling the need to reduce the overall environmental impact associated to human activities, particularly concerning energy consumption and carbon dioxide ($CO_2$) emissions. In this context, the building sector, accounting for over one-third of the overall energy demand worldwide is expected to reduce its environmental footprint to avert the expected 50% rise in energy demand before 2050 [1].

All this considered, in recent years, several research contributions worldwide have been focusing on the positive effect of passive techniques for building applications, foremost the use of building insulation materials [2, 3, 4, 5], or avant-garde design solutions such as ventilated facades [6, 7] and advanced ceilings or roofs configurations [8, 9, 10], which allow to reduce heat transfer through the building envelope.

In this context, the use of thermal energy storage (TES) materials, being capable to store heat to be later used under varying temperature conditions in combination with passive and active techniques has lately gathered increasing attention by the scientific community [11, 12, 13]. As a matter of fact, this kind of materials can guarantee a favorable dynamic response to the local boundary conditions, providing huge energy densities and, eventually, a unique buffering effect on indoor thermal fluctuations. In particular, latent thermal energy storage (LTES), above all in the form of phase change materials (PCMs), is nowadays considered a very promising field in both passive and active building applications.

Phase change materials can roughly be divided in organic and inorganic typologies. The former is usually distinguished in paraffin and non-paraffin, i.e. fatty acids, esters and alcohols, the latter in salt hydrates, salt compositions and metal alloys [14, 15, 16]. Although inorganic PCMs are usually

associated with better thermodynamic properties, they also possess high-volume change and supercooling effect, and because of this, carbon blends are generally preferred to be incorporated in low-temperature building applications [14]. In particular, organic PCMs with a phase change temperature between 30 and 70°C are generally used in solar thermal energy storage applications [17, 18], while temperature swings within the indoor environment of a building are usually dampened using melting points in the range 20-30°C [19].

In this respect, Brancato et al. [20] carried out an extensive DSC and stability characterization of the most attractive commercial PCMs and neat chemical compounds operating in the temperature range between 80°C and 100 °C. de Gracia et al. [21], on the other hand, developed and monitored the thermal performance of a ventilated façade with macro-encapsulated PCM under mechanical and natural ventilation, registering a 20% reduction in the electrical energy consumption of the installed HVAC system.

Several contributions also investigated the possibility of incorporating latent media within the stratigraphy of a building wall or ceiling. Shilei et al. [22], for example, analyzed the thermophysical effect of the integration of PCM within gypsum wallboards under winter climate conditions in southeast China. They found that the PCM wallboards alleviated indoor temperature fluctuations by approximately 1.15°C compared to ordinary wallboards. Similarly, Konuklu and Paksoy [23] incorporated PCMs with melting points of 26°C and 23 °C within sandwich panels and tested them under Mediterranean climatic conditions in Adana, Turkey, while D'Alessandro et al. [24] carried out an extensive thermo-mechanical investigation of the performance of innovative concretes produced by using 1, 3 and 5wt% of PCM micro- and macro-capsules in the final mix design of the composites.

Based on these and other literature contributions, it can be safely stated that phase change materials represent an excellent solution to dynamically meet the thermal-energy need of the building sector. In general, organic PCMs are characterized by unique thermal properties such as congruent melting and narrow melting/freezing temperature range, and because of this, they are considered the most suitable solution for cooling/heating applications in buildings [25, 26]. However, their relatively sharp transition range can be regarded as a limitation for their introduction in passive building envelope applications, where they could only be used to design case- and

seasonal-specific components.

Additionally, the most common materials used in latent applications, are still quite expensive on a practical basis and on top of that, they are often produced by using non-renewable raw materials, e.g. constituents from the petrochemical industry. Therefore, several researchers worldwide put forward the production of cheap renewable alternatives to replace petrochemically-derived media within the marketplace as the future road-map in thermal energy storage applications. In particular, innovative molecules from low cost vegetable oil feedstocks, and animal fats are nowadays being closely monitored [27, 28, 29, 30, 31].

In this context, Raghunanan et al. [32] analyzed the thermal stability of three template diester systems under both inert and oxidative environments using thermogravimetric analysis (TGA). They found that saturated and unsaturated diol derived diesters and saturated dibasic diesters can be used in a wide range of applications as high as their evaporation point, which was found to be above 240°C in all instances. Nikolič et al. [33], on the other hand, investigated the thermal stability of four different fatty acid esters: methyl stearate, methyl palmitate, cetyl stearate, cetyl palmitate and their binary mixtures, by using extensive DSC measurements and specifically developed thermal cycling. Results showed that the relevant thermophysical properties of the selected materials did not change in time.

This kind of frontier research, particularly focused on the investigation of more sustainable latent-based solutions, led to the development of a new category of phase change materials, i.e. the so called bio-based PCM. Bio-based PCMs are organic mixtures obtained from underused raw materials, such as soybean, coconut and palm oil, or even pork lard or tallow. They show huge latent heat, interesting chemical stability and can be manufactured such that their melting point can vary between -23 and 78 °C [34].
In this context, Wi S. et al. [35] used coconut oil and palm oil to prepare form-stable organic fatty acid ester PCMs with exfoliated graphite nanoplatelets (xGnP), while Noël J.A. et al. [19] conducted a life cycle analysis on two organic, biosourced PCMs, i.e. dodecanoic acid produced from palm kernel oil and and ethyl hexadecanoate produced from algae, focusing on their embodied energy and $CO_2$ emissions.
These and a few other scientific contributions demonstrate the urgent need of developing an advanced and low impact material for latent applications. However, most of these studies tend to manipulate the biosource with the aim of improving its thermophysical behavior and producing high-performance

substitutes for common PCMs such as paraffin, consequently and unavoidably increasing its embodied energy.

In this work, a novel bio-based PCM largely available on the market, having transition temperature in the ambient range is characterized, i.e. expired palm oil from food industry. Being recently partially withdrew from the food market as a consequence of scientific findings underlying its potential damage for human health [36], huge amounts of this material are currently stagnating in the food industry, eventually turning to waste upon expiring. Unsuitable as it may be for food applications, expired palm oil could still represent a sustainable application for non-specialized passive energy storage systems, where its dual-activated thermal behavior could represent a win to win solution for seasonal heat storage components. All this considered, a multipurpose thermal-based investigation was carried out on this material using thermogravimetric analysis (TGA), differential scanning calorimetry (DSC), thermal cycling and thermal monitoring during imposed hygrothermal cycles, with the aim of investigating its potential use in passive building envelope applications. Furthermore, the most important kinetic parameters were also analyzed to accurately predict the fire behavior of the palm oil together with its fire-resistance capability. Therefore a kinetic analysis was performed for defining the complete kinetic triplet, i.e. activation energy, pre-exponential factor and reaction model [37]. These results could be used in a CFD tool, such as Fire Dynamic Simulator (FDS), to carry out fire predictions on real scale [38].

## 2. Materials and methods

### *2.1. Phase change materials*

In this work, an innovative bio-based PCM encountering phase transition around the ambient temperature, was selected and investigated by means of (i) thermogravimetric analysis (TGA) (ii) differential scanning calorimetry (DSC), and (iii) extensive thermal monitoring in dynamic conditions. Results from the TGA were later used for investigating the kinetic of the thermal oxidation and defining the most proper reaction model. The selected PCM, i.e. expired palm oil from the market, was provided by a local bakery shop. The free fatty acid (FFA) profile of the blend, given in Table 1, was defined by means of gas chromatography (GC) analysis. In particular, a Varian 3300 instrument equipped with flame ionization detector and a TraceGold TG-Wax MS separation column from Thermo Fisher (30.0m$\times$0.25mm$\times$1.2$\mu$m)

was used. The injection volume was 1 $\mu$L, the split ratio was 1:50 and the inlet and detector temperatures were 250 and 260°$C$, respectively. GC chromatograms of the standards (procured from Sigma-Aldrich, USA) and samples were obtained under the conditions specified above 60 min run time.

Table 1: Fatty acid composition of the palm oil.

| Name | Structure | Composition [wt%] |
|---|---|---|
| Oleic acid | C18:1 | 38.1 |
| Linoleic acid | C18:2 | 10.1 |
| Palmitic acid | C16:0 | 43.0 |
| Stearic acid | C18:0 | 5.6 |
| Myristic acid | C14:0 | 1.4 |
| Lauric acid | C12:0 | 0.2 |
| Others | – | 1.6 |

### *2.2. Experimental methods for the multipurpose thermal investigation*

#### *2.2.1. Thermogravimetric analysis*

The palm oil thermal stability was evaluated by means of a thermogravimetric analyzer (Leco TGA601, Leco Corporation, MI, USA). TGA tests were carried out from about 303 K to 973 K in synthetic air, with a 3.5 L·min$^{-1}$ flow rate. As for the kinetic analysis, four heating rates below 20 K·min$^{-1}$ were used (5, 7, 10 and 15 K·min$^{-1}$), according to the ICTAC recommendations [39]. in each case 0.2 g palm oil were used to reduce both mass and heat transfer limitations [40]. Therefore, thermogravimetric (TG) and differential thermogravimetric (DTG) curves were obtained and initial decomposition and peak temperatures were determined. The initial decomposition temperature ($T_i$) and the peak temperature ($T_p$) were defined as the temperature at which 5% of the initial mass is lost and the temperature corresponding to the maximum thermal decomposition rate, respectively [41]. Blank tests were also carried out for TG baseline correction. Each thermal analysis was repeated twice to check the actual reproducibility of the tests.

#### *2.2.2. Kinetic evaluation by using isoconversional methods*

The palm oil trmal stability was evaluated by the calculation of the kinetic triplet, namely the activation energy (E), the reaction model f($\alpha$) and the pre-exponential factor (A). The decomposition rate is given by Equation (1) [39]:

$$\frac{d\alpha}{dt} = k\left(T\right) f\left(\alpha\right) h\left(P\right) \tag{1}$$

where t is time, T is the temperature, k(T) is the temperature dependence of the rate constant, f($\alpha$) is the differential form of the reaction model, h(P) is a function of the total pressure of the system (here neglected since it generally has low impact and is also usually ignored in most kinetic computational methods used for thermal analyses) [39]. The term $\alpha$, finally, is the conversion degree, expressed as:

$$\alpha = \frac{m_i - m_t}{m_i - m_f} \tag{2}$$

where $m_i$ is the initial mass of the sample (kg), $m_t$ is the mass of the sample at temperature T (kg), $m_f$ is the final mass of the sample (kg). The rate constant k(T) is defined by Arrhenius equation:

$$k\left(T\right) = A \exp\left(-\frac{E}{RT}\right) \tag{3}$$

where E ($kJ \cdot mol^{-1}$) is the activation energy, A ($s^{-1}$) is the pre-exponential coefficient and R ($J \cdot mol^{-1} \cdot K^{-1}$) is the universal gas constant. Considering non-isothermal runs at a heating rate, $\beta$=dT/dt, Equation (1) can be rewritten as follows:

$$\frac{d\alpha}{dt} = \frac{A}{\beta} \exp\left(-\frac{E}{RT}\right) f\left(\alpha\right) \tag{4}$$

Then by integrating Equation (4), Equation (5) is obtained:

$$\int_0^\alpha \frac{d\alpha}{f(\alpha)} = g(\alpha) = \frac{A}{\beta} \int_{T_0}^{T} \exp\left(-\frac{E}{RT}\right) dT = \frac{AE}{\beta R} p(u) \tag{5}$$

where p(u), with $u = E \cdot RT^{-1}$, and g($\alpha$) are the temperature integral and the integral form of the reaction model, respectively.

In this study, Starink [42] and Miura-Maki [43] distributed activation energy models were employed for the calculation of the activation energy as a function of the conversion rate. The isoconversional models are based on the following approximated linear equations:

$$\text{Starink: } \ln\left(\frac{\beta}{T^{1.92}}\right) = -1.0008\frac{E}{RT} + constant \tag{6}$$

$$\text{Miura-Maki: } \ln\left(\frac{\beta}{T^{2}}\right) = \ln\frac{A}{RE} + 0.6075 - \frac{E}{RT} \tag{7}$$

The activation energy can be determined by the slope of the regression lines of ln ($\beta$/$T^{1.92}$) vs. 1/T for Starink method and ($\beta$/$T^2$) vs. 1/T for Miura-Maki method.

*2.2.3. Master-plots method*

Master-plots method was applied in order to obtain the reaction mechanism and the pre-exponential factor of the palm oil thermal degradation process. For this purpose, Doyle's approximation [44] was employed in the temperature integral, p(u):

$$p\,(u) = 0.00484e^{-1.0516u} \tag{8}$$

In Equation (5), the determination of the pre-exponential factor is affected by the reaction model g($\alpha$); therefore, adopting a conversion reference point ($\alpha = 0.5$) Equation (5) becomes as follows:

$$g\,(0.5) = \frac{AE}{\beta R}p\,(u_{0.5}) \tag{9}$$

where $u_{0.5}$ = E/$RT_{0.5}$, $T_{0.5}$ is the temperature at $\alpha$=0.5 and g(0.5) is the integral form of the reaction model at $\alpha$=0.5. By dividing Equation (5) by Equation (9), the integral master-plots equation was obtained.

$$\frac{g\,(\alpha)}{g\,(0.5)} = \frac{p\,(u)}{p\,(0.5)} \tag{10}$$

By plotting the theoretical, g($\alpha$)·g(0.5)$^{-1}$, and experimental, p(u)·p(0.5)$^{-1}$, master-plots as a function of the conversion degree, the kinetic model which better describes the thermal decomposition reaction was determined. According to Yang et al. [45], the minimum standard deviation criterion was adopted for the determination of the acceptable kinetic model, as reported in Equation (11):

$$\Sigma\delta = \sqrt{\frac{\sum_j^n \sum_i^m \left[\frac{g_k(\alpha_i) p_j(u_i)}{g_k(0.5) p_j(u_{0.5})}\right]^2}{(n-1)\,(m-1)}} \tag{11}$$

where k, m, n are the serial number of the model functions shown in Table 2, the numbers of points and heating rates, respectively.

*2.2.4. Differential scanning calorimetry*

The thermophysical characterization was carried out with a differential scanning calorimeter (DSC 822e from Mettler Toledo) to analyze the phase change temperature and the phase change enthalpy of the blend. Two different reference standards (Indium at low temperature and Zinc at high temperature) were used for calibrating the DSC. The measurements were done with a three-cycle program. Results from the first cycle were disregarded, while the others were used for calculating the average phase change enthalpy with a confidence interval of 95%. The cycling was done at 5 K·min$^{-1}$ under flowing 80 mL·min$^{-1}$ nitrogen gas. The DSC were performed between 253.2 and 333.2 K with a mass sample of around 5 mg located in 40 $\mu$L aluminium crucibles. The equipment accuracy was $\pm$0.1 K for temperature and $\pm$3 kJ·kg$^{-1}$ for enthalpy.

*2.2.5. Thermal cycling stability*

An accelerated thermal cycling experiment was carried out to investigate the thermal stability of the blend, looking for eventual phase change temperature or enthalpy variations appeared after 100, 1000, and 10000 cycles. PCM samples were cycled in a thermal cycler Bioer Gene Q T-18 using 0.5 mL tube volume. A dynamic method using a temperature range between 293.2 K and 323.2 K at 4 K·s$^{-1}$ for both cooling and heating was established an used. DSC analyses were repeated upon cycling and the obtained results compared to the original values for comparison purposes.

*2.2.6. Thermal monitoring in dynamic conditions*

Besides the material characterization by means of TGA and DSC techniques, in this work, palm oil thermal performance were also evaluated during controlled heating and cooling processes using an ATT DM 340 SR climatic chamber, which allows to control the temperature condition of a 601×810×694 mm$^3$ test compartment in the range 233÷453 K.

More in detail, three palm oil samples were produced by pouring the bio-based PCM in three identical cylindrical sample holders made of glass (each of which with a volume of about 1385 $cm^3$), and housed within the test compartment of the ATT DM 340 SR equipment. A thermal cycle characterized by three temperature plateaus (two at 268.2 K and one at 333.2 K) interspersed with two linear steps (an increasing and a decreasing temperature ramp with a heating rate of about 0.2 $K \cdot min^{-1}$) was designed in order to first trigger the melting and then the crystallization of the investigated material (see Figure 1.a). The temperature forcing procedure was specifically realized with the aim of investigating the thermal response of the material considering temperature ranges that typically characterize real applications, in order to investigate its possible behavior when integrated in engineered building components.

The thermal response of the samples was continuously monitored over the entire length of the 20 hours-long cycle (with a sampling time of 20 seconds) by means of 27 T-type thermocouples (9 per sample), with an accuracy of 0.5 K. The temperature sensors were placed in three different positions along the diameter of each cylinder, i.e. 1, 3.5 and 6 cm away from the side surface of the cylinder, at three different heights, i.e. 1, 3.5 and 6 centimeters away from the lower surface of the cylinder (see Figure 1.b).

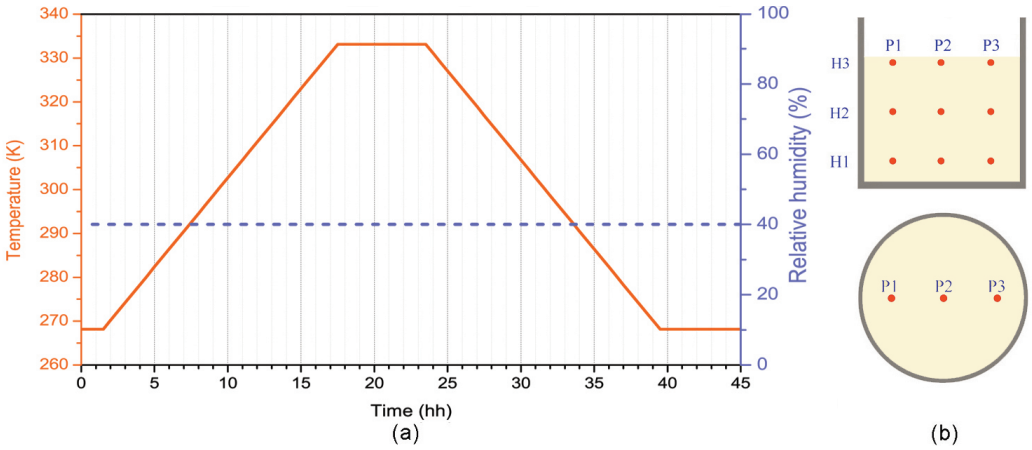


Figure 1: (a) Imposed thermal cycle and (b) thermocouples positioning within the palm oil sample.

### *2.3. Life cycle assessment*

#### *2.3.1. Goal and scope definition*

After completing the thermal investigation of the palm oil as described in Section 2.2, a life cycle assessment (LCA) approach was applied to the same material, according to the international standards of the ISO 14040 series [46, 47]. The primary objective of this study was to determine and evaluate the environmental impacts of the bio-based PCM and compare them with those of common products from the petrochemical industry, i.e. paraffin.
As described in Section 1 and 2.1, the palm oil selected in this work is a residual product from the local market, which was recently partially withdrawn from the food industry due to its potential damages to the human health [36]. Such an abrupt variation in the market demand caused the stagnation of the residual product and paved the way for its potential alternative applications. All this considered, two different scenarioes were analyzed in terms of palm oil environmental impacts: the former (POraw) considers the product as a raw material and takes into account all the impacts deriving from its cultivation and production, while the latter (POwaste) assumes the palm oil to be a waste from the food industry, thus, according to the polluter pays principle introduced in the Product Category Rules (PCR) for contruction products and services [48], all the impacts due to the upstream processes are imposed to zero.

Additionally, given the innovativeness of this application, and because there are no exhaustive data available about the use of the palm oil as a PCM in a real building, a cradle-to-gate LCA approach was employed. In particular, the following life-cycle steps were analyzed for the POraw approach:

- Palm tree cultivation;
- Crude palm oil production;
- Transports along all phases.

Concerning the POwaste approach, all the impacts deriving from the palm cultivation and the crude palm oil production and the related transports are imposed to zero. Therefore, only the transport between the food industry and the place of final application is taken into account.
According to ISO 14040 standard, a reference functional unit (f.u.) must be

defined for properly quantifying the environmental performance of the system. The functional unit (f.u.) of the present LCA study was defined as the mass in kg of material (palm oil or paraffin) that must be used to guarantee the same specific latent heat of fusion in the temperature ranges 3–6°C and 26–34°C, i.e. 33 kJ·kg$^{-1}$ and 14 kJ·kg$^{-1}$, respectively. This functional unit gives information about the amount of latent material required to obtain a specific heat of fusion during the identified phase change processes. It is particularly appropriate since the environmental impacts associated to the materials have been investigated with regard to latent contribution to the heat transfer that the material will guarantee in a real application.

Of course, both the palm oil scenarios consider 1 kg of material. Concerning the paraffin, since all commercialized products guarantee a unique fusion range, two different PCMs with a melting temperature centered in each of the specified fusion ranges were selected and used. In particular, RT4 paraffin with a specific latent heat of fusion of 173 kJ·kg$^{-1}$ and RT31 paraffin with a specific latent heat of fusion of 163 kJ·kg$^{-1}$, produced by Rubitherm were considered [49, 50]. Therefore the f.u. for the paraffin is 0.28 kg, i.e. 0.19 kg of RT4 and 0.09 kg of RT31. The obtained results are resumed in Table 2.

Table 2: Specific latent heat of fusion at 277K, i.e. 4°C ($L_{H,277}$) and at 304K, i.e. 31°C ($L_{H,304}$), and functional unit (f.u.) of the different materials considered.

| Material | Component | $L_{H,277}$ [kJ·kg$^{-1}$] | $L_{H,304}$ [kJ·kg$^{-1}$] | f.u. [kg] |
|---|---|---|---|---|
| Palm oil | Palm oil | 33 | 14 | 1 |
| Paraffin | RT4 | 173 | - | 0.19 |
| | RT31 | - | 163 | 0.09 |

*2.3.2. Preliminary assumptions and limitations*

As previously said, the use phase (integration of the PCM-based panel in the selected application, e.g. the building envelope) was not included in the system boundaries of this LCA study, for lack of information due to the innovative nature of the study. The related environmental impacts were hence neglected, considering a cradle to gate approach. Some further assumptions for this LCA are the following:

- The data used for the inventory phase, were not based on questionnaires answered by the palm oil manufacturer but were taken from databases

available in SimaPro 8.3. However, since these databases were implemented considering a large number of palm oil production chains, they can be taken as an acceptable reference value for this study.

- The study is limited to the previously described system boundaries.

- The environmental impact assessment is limited to the categories taken into account in three life cycle impact assessment methods: the ReCiPe 2008 method, the Cumulative Energy Demand method (CED) and the Intergovernmental Panel on Climate Change method (IPCC) [51].

- Similar packaging was assumed for producing the palm oil and paraffin macrocapsule for this reason, the impacts deriving from these stage were not taken into account in the final comparison.

*2.3.3. Life cycle inventory (LCI)*

In this work, the environmental performance of expired palm oil from food industry when used as a phase change material were evaluated and compared to those of a more common latent thermal energy storage solution, i.e. paraffin. Two different palm oil scenarios were investigated: POraw (which considers the product as a raw material) and POwaste (which assumes the palm oil to be a waste from the food industry). All the processes considered in this LCA study were chosen to be global averages, and consider the attributional approach in which burdens are attributed proportionally.

The inventory phase was carried by using the SimaPro software, version 8 and the ecoinvent database version 3. Both the POraw and the POwaste scenario were implemented by adapting the "Palm oil, refined GLO - market for - Alloc Def" process from the ecoinvent database, with the addition of a further transport process from the food industry to the new development site, where the material is supposed to be gathered and transformed into a macro-encapsulated panel for civil applications. This final transport stage is assumed to be carried out by using a 10 ton lorry and considers a distance of 400 km, which was chosen as a representative average value for transportation in Italy.

The LCA study carried out for the common phase change material for comparison purposes, was implemented considering the "Paraffin GLO- market

for- Alloc Def" process available in the ecoinvent database. Since this particular process is general for paraffin production, the sum of the two different PCMs was modeled in a unique process considering the sum of RT4 and RT31. It is noteworthy, finally, that the packaging procedure is assumed to be the same for both the palm oil and the paraffin, so its environmental impact is here always neglected.

## 3. Results and discussions

### *3.1. Thermal decomposition characteristics*

Thermal stability of vegetable oils is mainly determined by the initial decomposition temperature that can be calculated with sufficient precision by using slow heating rates (lower than 5 K·min$^{-1}$) [52]. Figure 2 shows TG and DTG curves of the palm oil under air atmosphere at the heating rate of 5 K·min$^{-1}$. In particular, the derivative profile can be divided into three oxidation stages, mainly related to the degradation of polyunsaturated, monounsaturated and saturated fatty acids [53].
The initial decomposition temperature is observed at 562 K and the first step ends at approximately 618 K, with about 25 wt.% of palm oil loss. At this stage polyunsaturated fatty acids, such as linoleic and linolenic acids, are decomposed and volatile compounds are produced and removed by vapor obtained during heating [39]. The second stage takes place in the range 618–718 K, during which volatilization of triglycerides, mainly composed of monounsaturated fatty acids occurs, and the peak temperature (680 K) is reached, confirming the high content of oleic acid in the analyzed bio-based PCM. At the end of this step only 8% of palm oil remains. The third and final stage of thermal degradation, registered between 718 K and 793 K, can be attributed to the volatilisation of saturated fatty acids (palmitic and myristic acids). The curve flattering at 793 K shows that no further decomposition takes place.

### *3.2. Determination of the activation energy*

Decomposition kinetics during the palm oil oxidation process are calculated by using Staring and Miura-Maki models at degrees of conversion ($\alpha$) ranging from 0.20 to 0.80 with a step of 0.05 according to the ICTAC recommendations [39]. This particular range is chosen in order to obtain more

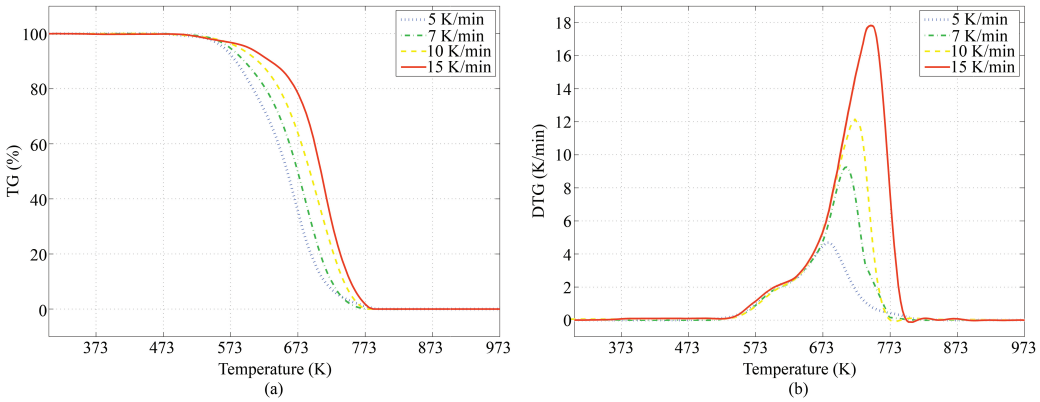


Figure 2: Thermal decomposition process of the palm oil sample at 5, 7, 10 and 15 K·min$^{-1}$: (a) TG curve, and (b) DTG curve.

precise kinetic data; in fact, for values below 0.20 multiple reactions can occur, while above 0.80 the experimental error can increase due to the negligible residue.

Table 3 shows the values of E and the correlation coefficient ($R^2$), calculated by using Equations (6) and (7). All the plots are characterized by high $R^2$ values, i.e. ranging from 0.9646 to 0.9995, demonstrating good fitting to the experimental results.

Differences between the Starink and Miura-Maki methods in terms of activation energy values are within 0.5% of the lower value, demonstrating that the results are acceptable. Furthermore, E values between 48.5–127.0 kJ·mol$^{-1}$ and 48.1-126.7 kJ·mol$^{-1}$ are obtained by the Starink and Miura-Maki methods for $\alpha$ values ranging from 0.2 to 0.8. The variation of E as a function of the conversion degree suggests that the decomposition of the palm oil is a complex reaction including parallel, competitive, consecutive and reversible reactions [54]. In particular, the rapid increase of activation energy in the range of conversion degree between 0.55–0.80 is due to the heat transfer at high temperatures [55]. The activation energy is a key factor for the determination of the thermal stability of samples since it represents the energy barrier to be exceeded to break the chemical bonds between atoms [56]. The obtained overall mean value of activation energy ($83 \pm 25$ kJ·mol$^{-1}$) for both methods) is lower than that calculated for other vegetable oils (146, 151, 144, 157 kJ·mol$^{-1}$ for mustard, soybean, olive and karanja oils, respectively [57]) during thermal decomposition in inert atmosphere. This result is

Table 3: Activation energies of palm oil at different degrees of conversion by using Starink and Miura-Maki methods.

| Degree of conversion ($\alpha$) | Starink method | | Miura-Maki method | |
|---|---|---|---|---|
| | E ($kJ \cdot mol^{-1}$) | $R^2$ | E ($kJ \cdot mol^{-1}$) | $R^2$ |
| 0.20 | 48.5 | 0.9941 | 48.1 | 0.9941 |
| 0.25 | 52.4 | 0.9936 | 52.1 | 0.9935 |
| 0.30 | 53.7 | 0.9993 | 53.3 | 0.9993 |
| 0.35 | 55.7 | 0.9995 | 55.3 | 0.9995 |
| 0.40 | 59.6 | 0.9995 | 59.2 | 0.9995 |
| 0.45 | 62.9 | 0.9976 | 62.5 | 0.9976 |
| 0.50 | 67.2 | 0.9851 | 66.8 | 0.9849 |
| 0.55 | 71.0 | 0.9677 | 70.6 | 0.9674 |
| 0.60 | 77.5 | 0.9708 | 77.1 | 0.9705 |
| 0.65 | 84.2 | 0.9649 | 83.8 | 0.9646 |
| 0.70 | 94.0 | 0.9700 | 93.6 | 0.9697 |
| 0.75 | 107.9 | 0.9787 | 107.5 | 0.9786 |
| 0.80 | 127.0 | 0.9784 | 126.7 | 0.9782 |
| Average | 83 | | 83 | |
| Standard deviation | 25 | | 25 | |

probably due to a higher content of impurities such as free fatty acids, mono- and diacylglycerols, phospholipids and oxidation products [58].

*3.3. Reaction model and pre-exponential factor determination*

The mean activation energy value, obtained by the isoconversional methods, was employed in the master-plots method in order to predict the reaction mechanism of palm oil. Since the E values obtained by Starink and Miura-Maki methods coincide, the average value of 83 $kJ \cdot mol^{-1}$) was selected for the evaluation of the reaction model. Figure 3 shows the theoretical, $g(\alpha) \cdot g(0.5)^{-1}$, and the experimental, $P(u) \cdot P(u_{0.5})^{-1}$, master-plots as a function of the conversion rate. As can be seen the experimental master-plots at different heating rates are almost identical, demonstrating that the thermal degradation process of palm oil could be described by a single kinetic model. Furthermore, by comparing the experimental with the theoretical curves, the kinetic model that best fits the experimental curves can be determined. Table 4 shows the values of the sum of standard deviation for various reaction models, calculated according to Equation (11). The most probable reaction

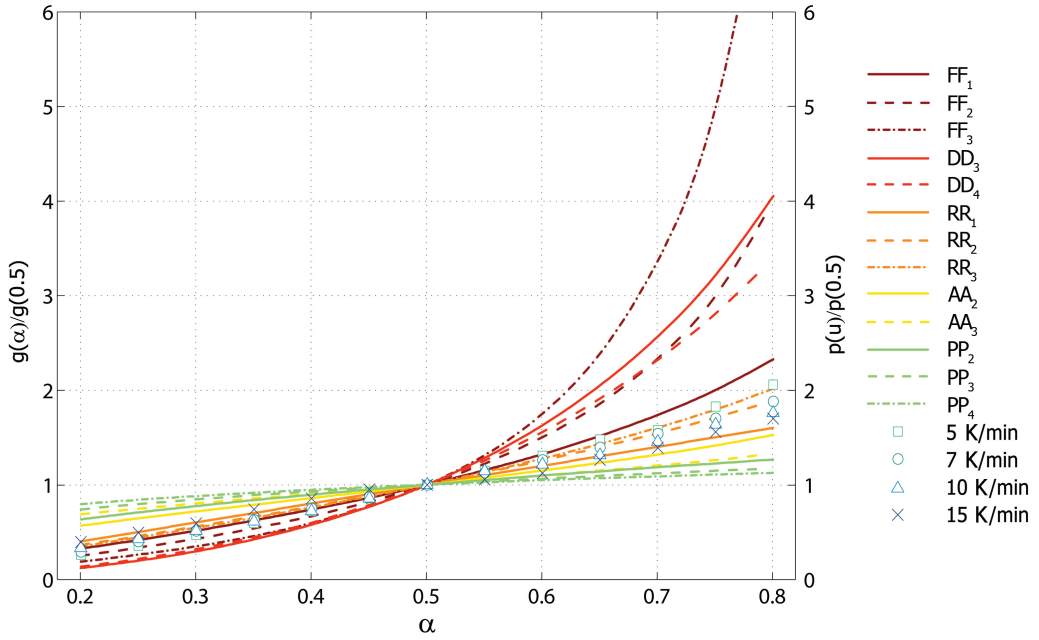


Figure 3: Plots for determination of activation energy at different conversion rates by (a) Starink method, and (b) Miura-Maki method.

model for the thermal decomposition of palm oil is the phase boundary controlled process (contracting area, $RR_2$ mechanism) in which the nucleation step occurs immediately, so that the surface of each particle is covered with a layer of the product [59].

The mathematical expression of the reaction mechanism was used to estimate the pre-exponential factor. The expression of $RR_2$ was inserted into Equation (5) obtaining Equation (12):

$$1-(1-\alpha)^{1/2}=\frac{AE}{\beta R}\rho\left(u\right) \tag{12}$$

where E is the average value of the activation energy (83 kJ·mol$^{-1}$).

At this stage, the values of the pre-exponential factor can be calculated from the slope of the straight line by plotting $[1(1\alpha)^{1/2}]$ versus EAp(u)·$(\beta R)^{-1}$ at various heating rates. From the results shown in Table 5, it can be noted that changes in the heating rate cause minimal difference in the values of A, confirming the single step reaction. The knowledge of the values of the pre-exponential factor is important because it describes the reaction chemistry

of the process. In particular, A values lower than $10^9$ $s^{-1}$ could indicate a surface reaction, however, if the surface area doesn't influence the reaction, low pre-exponential factor values may also represent a tight complex [60]. The kinetic triplet (E, A, and f($\alpha$)) for the investigated thermal decomposition process of the palm oil can also be employed to define the kinetic expression using Equation (4). Therefore, Equation (13) can describe the kinetic reaction in a single-step for palm oil.

$$\frac{d\alpha}{dt} = 2.66E + 08 \exp\left(-\frac{72850}{RT}\right)\left[2(1-\alpha)^{1/2}\right] \tag{13}$$

Results from the thermal analysis can be used to investigate thermal aging of materials, i.e. the time-dependent decay produced by heat exposure. Said aging can of course be influenced by other factors, such as mechanical stress, moisture, exposure to sunlight and air, etc. However, if the palm oil is used for building or similar applications as an additional layer within a more complex stratigraphy, heat can be assumed as the main cause of aging. In this context, equation (13) is useful to estimate the lifetime ($t_f$) of palm oil that undergoes thermal aging, which is defined as the time period after which the material undergoes a change in its properties that it can no longer satisfy the function for which it was produced [39]. In particular, the degradation time ($t\alpha$) required to reach a given conversion rate can be calculated by Equation (14), which is the integral of Equation (13).

$$t_\alpha = \frac{1-(1-\alpha)^{1/2}}{2.66E + 08 \exp\left(-\frac{7285}{RT}\right)} \tag{14}$$

The lifetime, $t_f$, is obtained from the Equation (14) assuming that the conversion rate is equal to 5%. Figure 4 shows the logarithmic curve of lifetime versus temperature for palm oil. Based on the calculation shown above, the lifetime of palm oil at 323 K and 373 K is equal to about $4.2\times10^9$, $9.6\times10^5$ years, respectively, demonstrating that palm oil can be employed in some applications where low to medium constant temperatures is required for a very long time without failure.

*3.4. Results from the DSC characterization before and after thermal cycling*

Figure 5 shows the results from the differential scanning calorimetry of the palm oil before the thermal cycling procedure. As can be seen, the bio-based PCM presents two different peaks both during the melting and the

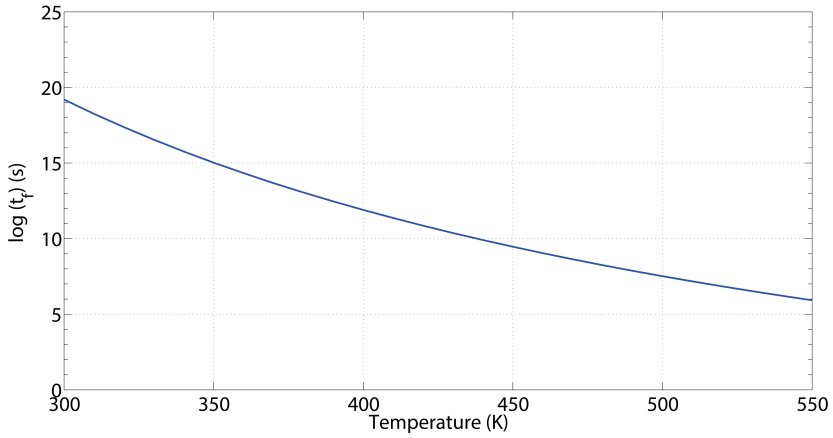


Figure 4: Logarithm of lifetime as a function of temperature for palm oil.

freezing process, due to its unique chemical composition, which was shown to be particularly reach in saturated and monounsaturated fatty acids. More in detail, before aging, the onset temperature of the first melting peak is observed at 264.4 ± 0.1 K (about -8.8 °C, while the melting peak is registered at 276.4 ± 0.1 K. As for the second peak, in this case the onset temperature is at about 24 °C, i.e. 297.2 ± 0.1 K, and the melting peak at 307.0 ± 0.1 K.

The solidification phenomenon, on the other hand, starts at about 20.9 and 5.2 °C (282.2 ± 0.1 and 278.4 ± 0.1 K), reaching the peak at about 19 and 3 °C, i.e. 292.3 ± 0.1 and 275.9 ± 0.1 K. Consequently, it can be stated that the palm oil is associated to a relatively high subcooling effect at the higher temperature peak, i.e. about 14.66 ± 0.17 K difference in the peak, while this phenomenon is basically negligible when the lower temperature transition is taken into account, i.e. about 0.55 ± 0.17 K difference in the peak. Said subcooling effect, most probably is a consequence of the main chemical composition of the palm oil. In particular, recent studies investigating TAGs–DAGs (triglycerides – diacylglycerols) interaction in palm oil during crystallization, showed that the latter have deleterious effect on the characteristics of this phenomenon [61, 62]. According to Watanabe et al. [63], the negative effect of DAGs on the crystallization of palm oil would be related to the low nucleation rate of TAGs in the presence of these compounds.

Concerning the latent heat of fusion of the bio-based PCM, they were cal-

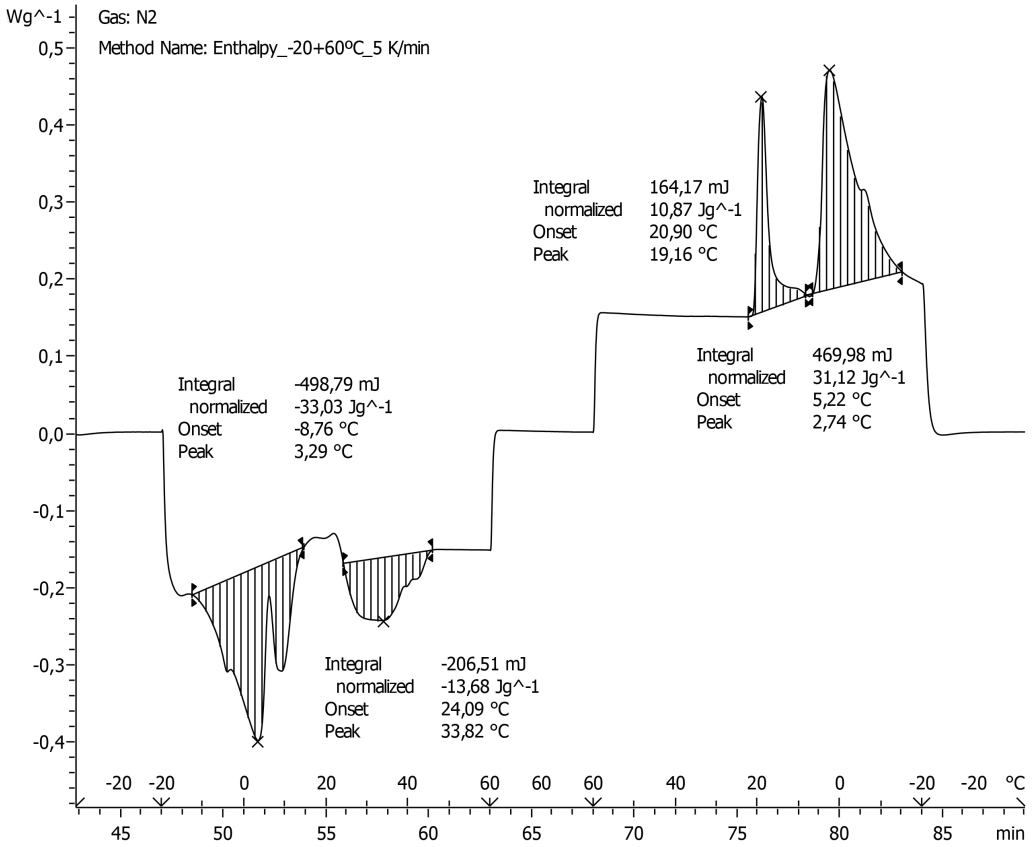


Figure 5: Palm oil DSC results.

culated by numerically integrating the areas under the peaks of phase transitions from solid to liquid and from liquid to solid states. According to the obtained results, the heat of fusion of the palm oil globally reaches 47 $\pm$ 5.2 kJ·kg$^{-1}$. This result, although lower than the most common commercial products [34], is still promising for a cost-effective, bio-based solution such as palm oil. Furthermore, the possibility of having a single material with two different activation temperatures represents an interesting application in terms of seasonal passive building envelope components. As a matter of fact, contrary to active latent applications, were highly collimated transition peaks ensure higher efficiency, in passive building envelope solutions, where wide daily and seasonal thermal oscillations generally take place, the palm oil thermal behavior could represent a promising low-cost and low-tech solution.

Table 6 also shows the values of the DSC analysis after the thermal cycling procedure. Said results show quite good performance of the bio-based PCM up to 1000 cycles. As a matter of fact, despite a general decrease of the melting enthalpy with increasing number of cycles can be detected, the maximum variation is 9.1% for the lower temperature peak, and 1.8 % for the higher temperature one. These variations increase up to 21.4 and 5.6 %, respectively, after 10000 aging cycles. As for the different onset temperatures registered for the melting process, they maintain a stable value up to 1000 cycles, while reaching a maxim deviation of about 1 degree after 10000 cycles. A more variable pattern can be found in the freezing process, where however, the subcooling effect plays a non-negligible role in the final stability of the blend.

*3.5. Results from the thermal monitoring*

Figure 6 shows the temperature profiles from the thermal monitoring of the investigated PCM during the imposed thermal cycle. The dashed line represents the local forcing imposed by the chamber, while the other ones represent the average temperature trends of the three palm oil samples at the three considered heights, i.e. H1 = 1 cm, H2 = 3.5 cm and H3 = 6 cm. As can be seen, each profile follows quite regularly the imposed thermal cycle, however, the H3 trend seems to be more rapidly affected by the local boundary conditions throughout the measurement. This is due to the fact that at this height the thermocouples are in close proximity of the surface of the samples, and because of this, they are highly influenced by the adjoining air volume conditions.
The H2 and H1 temperature profiles, on the other hand, are essentially overlapping during the whole duration of the cycle, and show unique deviations during both the heating and the cooling ramp. These deviations from the imposed temperature forcing are a consequence of the latent phenomena taking place in the palm oil matrix.
In order to more carefully investigate the thermal performance of the bio-based blend and identify the temperature ranges at which the phase transitions take place, each temperature trend was numerically investigated and the global maxima and inflection points calculated.

More in detail, as can be seen in Figure 7 and Table 7, the maximum temperature value, i.e. about 333.5 K is firstly reached by the superficial layer of palm oil, then by the lower and the central one, i.e. after about 22 hours and 59 minutes, 23 hours and 0 minutes and 23 hours and 08 minutes,

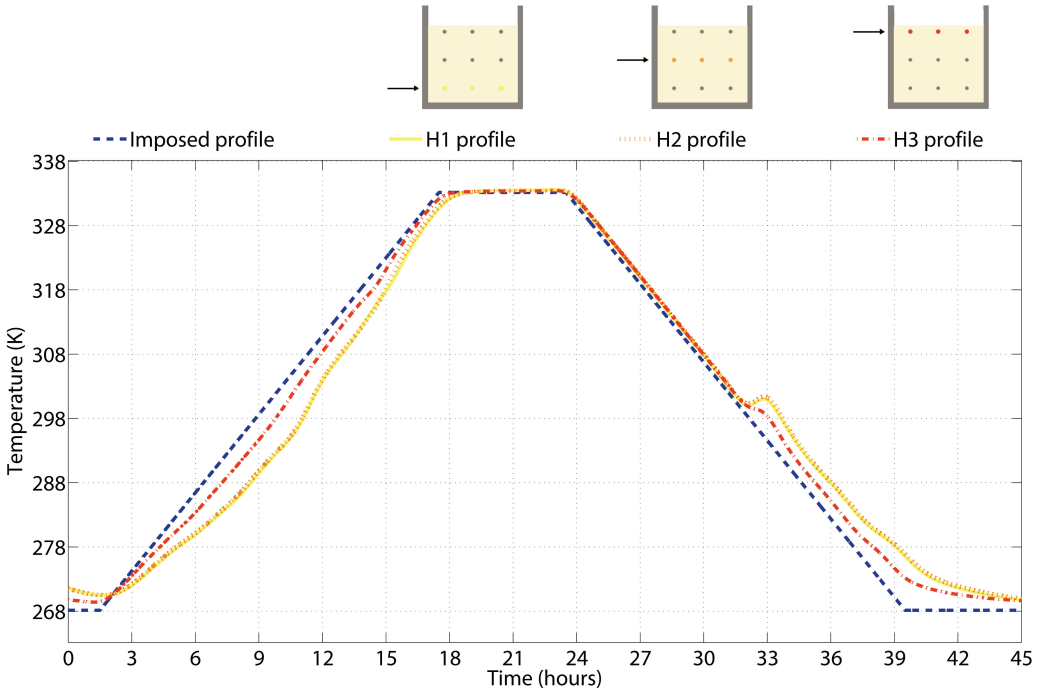


Figure 6: Palm oil average thermal profiles at the three considered heights.

respectively.

Concerning the concavity behavior of the monitored profiles, each temperature trend shows four inflection points both during the heating and the cooling ramp imposed by the chamber. The temperature value of these points is very similar and allows to define two different melting transitions, i.e. the first one in the temperature range 274.7 – 279.4 K, the second between 301.0 and 314.0 K, and two different crystallizations, i.e. in the range 307.8 – 292.0 K and 286.4 – 277.1 K.

Consequently, the detrimental subcooling effect, already detected by the DSC analysis, although less pronounced, was also found in the dynamic monitoring procedure.

### *3.6. Life cycle impact assessment*

#### *3.6.1. ReCiPe 2008*

Figure 8 presents the results of the comparative LCA analysis of the palm oil considered as a raw material (POraw), the waste palm oil (POwaste) and

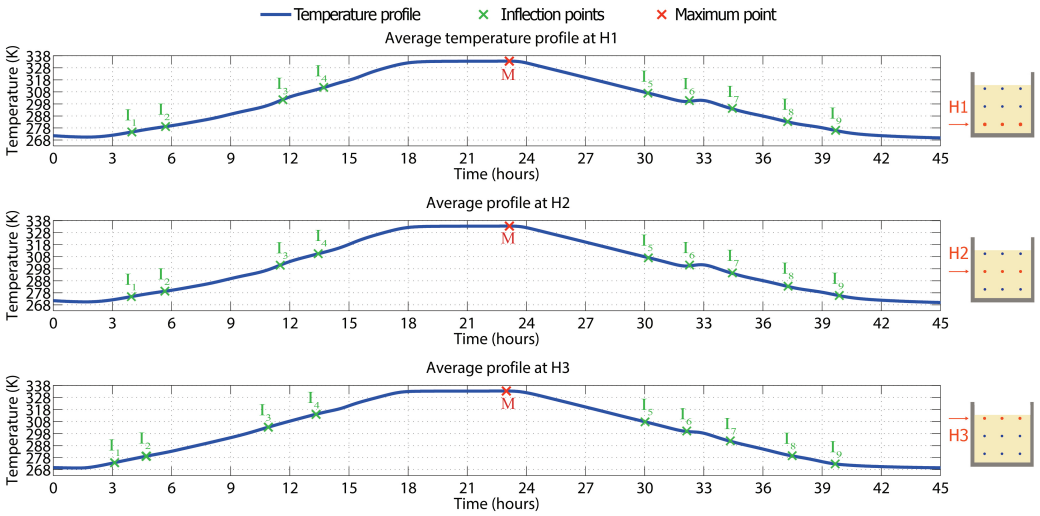


Figure 7: Palm average thermal profiles with the specific maximum and inflection points.

the paraffin through the ReCiPe 2008 method. The unit of measure in the ReCiPe method is the "point" (here millipoint, mPt), which represents the total environmental load expressed as a single score. In this score, characterization, damage assessment, normalization and weighting are combined for allowing a direct comparison among the different impact categories [64]. As can be seen, the production of the palm oil produces the highest impacts on the ecosystem and human health, i.e. about 170 and 104 mPt, while the paraffin takes the lead when in terms of resources depletion, being associated to a final score of about 37.5 mPt against the 15.5 mPt of the raw palm oil. Globally, the POraw scenario is the one that is associated to the highest environmental impact, and this is manly due to the emissions and land and water consumption associated to the palm tree cultivation.
Concerning the POwaste scenario, the environmental impact assessment is in this case particularly low, never exceeding 3 mPt in any of the three macro categories of the ReCiPe method. As expected, fossil fuel depletion and climate change human health show the highest burden as far as the POwaste is taken into account. This is of course a consequence of solely considering the impacts deriving from the final transportation stage, according to the polluter pays principle as described in Section 2.3.1.

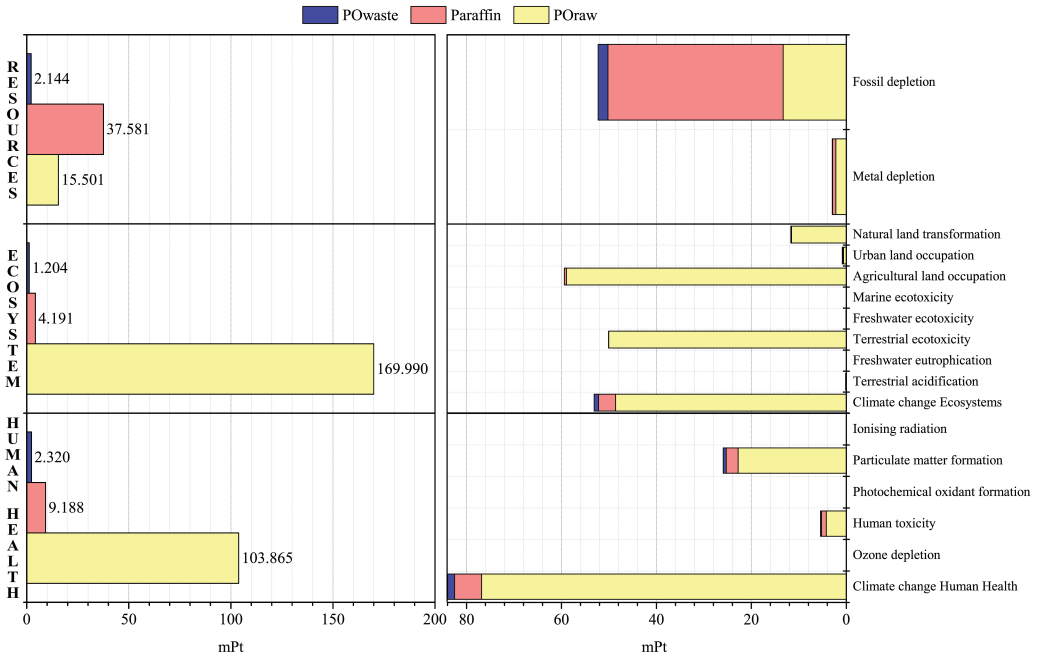


Figure 8: LCA results with respect to the ReCiPe impact categories and macro-categories.

### *3.6.2. Cumulative energy demand (CED)*

Concerning the primary energy consumption once again the best results are those of the POwaste scenario, which globally accounts for about 0.878 MJ, most of which are associated to non fossil depletion (see Figure 9). As for paraffin and POraw scenario, they produce much higher and similar global impacts, i.e. 15.419 and 17.347 MJ, respectively. However, the impact of paraffin is mainly associated to the non-renewable fossil depletion category, while the palm oil higher effect can be found in the renewable biomass category (8.665 MJ), followed by the non-renewable fossil and the non-renewable biomass categories (5.42 and 2.367 MJ, respectively).

### *3.6.3. Intergovernamental panel on climate change (IPCC)*

Concerning the climate change factors of IPCC, in this work we considered the time-frame of 100 years (GWP 100a method). Results in Figure 10 show the huge footprint of the palm oil complete production chain, i.e. 2.772 $kgCO_2eq$, when compared to the paraffin 0.207 $kgCO_2eq$. It is noteworthy, however, that when the POwaste scenario is taken into account, the emissions of palm oil are reduced to 0.053 $kgCO_2eq$. Based on these results, it is

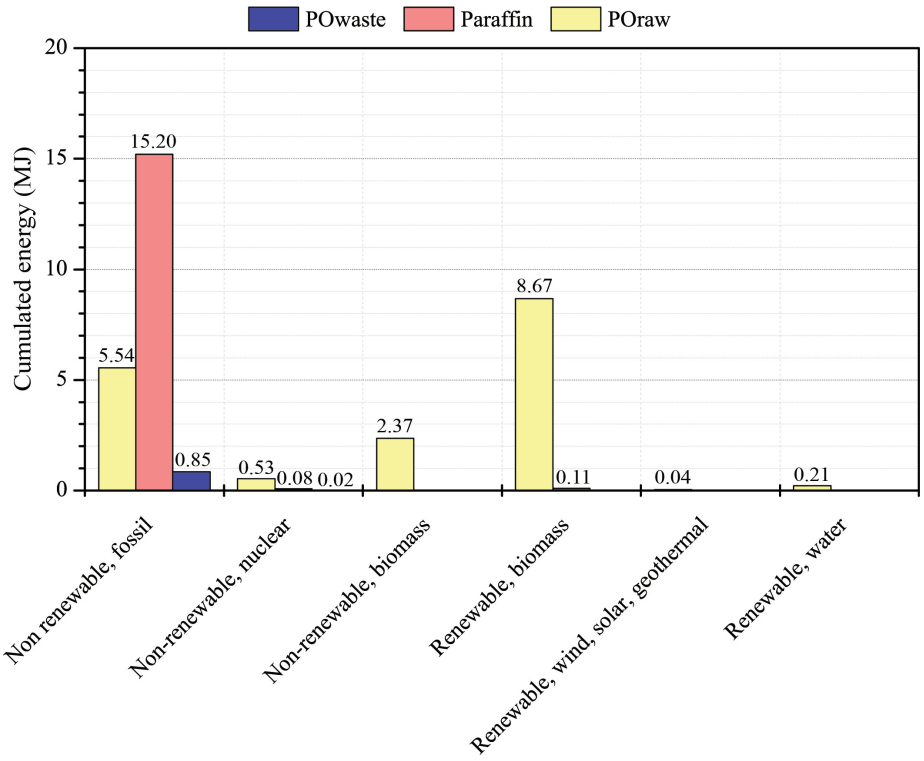


Figure 9: LCA results with respect to the 6 CED impact categories.

clear that, as in the previous assessment methods, the highest impacts are mainly related to the palm tree cultivation and oil extraction, while the final transportation produces a significantly lower environmental footprint.

*3.7. Life cycle interpretation*

In this work, the potential environmental foot print of expired palm oil from the food industry, when used as phase change material, is investigated and compared to a more common petrochemical-based solution, i.e. paraffin. As expected, results from each of the assessment methods used in this analysis show the huge impact of raw palm oil, particularly in terms of damages to the ecosystem and the human health. As a matter of fact, in the ReCiPe method, palm oil shows more than five times the impacts of paraffin, while in the IPCC, its impacts are ten times as big as those of the petrochemical product. A lower difference is found in terms of primary energy consumption (CED method), although the raw palm oil is still identified as the most

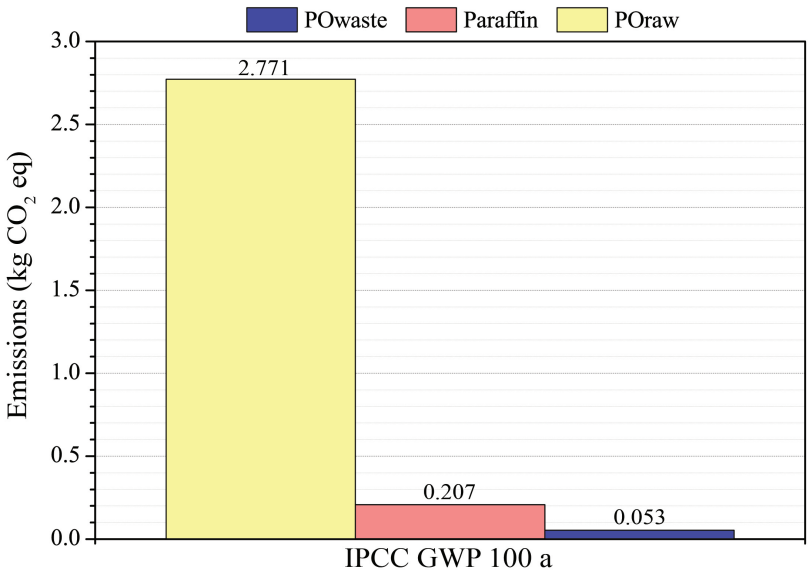


Figure 10: LCA results with respect to the IPCC method.

damaging solution.
This is of course a consequence of the huge environmental burden due to the palm oil cultivation process. Indeed, most of the impacts (about 81%), are associated to the categories of climate change, agricultural land occupation and terrestrial ecotoxicity.
Precisely based on the awareness that the development of new plantations, coupled with the expansion of smallholders farms has resulted in significant deforestation, and on the potential damage for human health [36], palm oil has been recently banished from the food industry. All this considered, huge amounts of this material often expire, and become, in effect, a waste material.

The environmental footprint of palm oil considered as waste, is of course much lower. In fact, since based on the polluter pays principle [48], all the impacts due to the upstream processes are imposed to zero, this scenario results in one order of magnitude lower impacts compared to paraffin, in each of the selected methods of assessment. Of course this is a simplification, of reality. It would be interesting to define a specific economic allocation to take into account the depreciation of the product, due to the established market trend.

## 4. Concluding remarks

In this work, a multipurpose investigation was carried out on a low cost bio-based phase change material from the local food industry, i.e. expired palm oil, using thermogravimetric analysis (TGA), differential scanning calorimetry (DSC), thermal cycling and extensive thermal monitoring during imposed thermal cycles. Additionally, an oxidation kinetic analysis was also carried out on the selected blend, to obtain useful information for combustibility and flame spread numerical models.

Results from the TGA show three different oxidation stages, associated to the thermal degradation of polyunsaturated, monounsaturated and saturated fatty acids. Average activation energies of 83 $kJ \cdot mol^{-1}$ were obtained using the Starink and Miura-Maki methods. Result from the kinetic analysis through Master-plot methods suggested that the palm oil thermal degradation can be described by the two-dimensional phase boundary reaction, while the lifetime investigation revealed an optimal thermal durability in medium-low temperatures applications. A numerical analysis is underway for the prediction of fire behavior of palm oil by using the kinetic parameters calculated in this study.

Concerning the DSC analysis, the investigated PCM showed two broad melting peaks, with onset temperatures at -8.8 and 24°C, with a melting enthalpy of about 33 and 14 $kJ \cdot kg^{-1}$, respectively. Additionally, a promising long term stability of the blend was observed combining DSC and thermal cycling after 100, 1000 and 10000 aging cycles. The same number of transitions was also registered in the thermal monitoring during the imposed thermal cycle, where four inflection points in the heating and five in the cooling ramp are shown, as a result of a non-negligible subcooling phenomenon taking place at the higher temperatures transition.
As for the environmental investigation, a general better behavior of the expired palm oil is noticeable, compared to the other products. This is because in this scenario, all the upstream processes are imposed to zero, based on the polluter pays principle.

In conclusion, this work showed that, despite the relatively low transition phase entalphy compared to chemical preparations already on the market, expired palm oil from the food stock could represent a promising material for non-specialized passive applications where wide thermal oscillations both at the seasonal and the daily scale are expected. Indeed, in these cases a

narrow transition interval, although highly efficient in a specific temperature range, reveals to be useless when said temperatures are not reached. In this context, the introduction of a latent product characterized by two distinct phase transitions can be considered as an avant-garde technology for simultaneously reducing winter dispersion and summer overheating. In particular, passive building envelope solutions, could very well benefit from the use of a low-tech and low-cost latent component, that, once integrated in the outer layers of the building envelope, would buffer indoor thermal fluctuations indiscriminately during winter and summer.
The here presented bio-based material represents a potential breakthrough in terms of life cycle building energy efficiency and promising developments in palm oil doping or optimization may be expected at a later stage of this experimentation.
This is all the more interesting, considering its low cost, simplicity, large availability, environmental friendliness, and the minimum risk even in case of leakage in the built environment.

Future studies should address the matter of increasing the palm oil energy storage density, possibly purifying the bio-based blend by means of low embodied energy procedures, while also investigating subcooling reduction to guarantee a more stable material for high performance and yet sustainable, seasonal building envelope solutions.

## Acknowledgment

This work was partially funded by the Ministerio de Ciencia, Innovacin y Universidades de Espaa (RTI2018-093849-B-C31). Dr. Cabeza would like to thank the Catalan Government for the quality accreditation given to her research group GREiA (2017 SGR 1537). GREiA is a certified agent TECNIO in the category of technology developers from the Government of Catalonia. This work is partially supported by ICREA under the ICREA Academia programme. Authors from University of Perugia thank Fondazione cassa di Risparmio di Perugia for supporting the investigation about biomaterials within the project SOS CITTÁ 2018.0499.026.

## References

[1] Transition to Sustainable Buildings - Strategies and Opportunities to 2050, Tech. rep., International Energy Agency (2013).

doi:10.1787/9789264202955-en.

[2] S. Schiavoni, F. D'Alessandro, F. Bianchi, F. Asdrubali, Insulation materials for the building sector: A review and comparative analysis, Renewable and Sustainable Energy Reviews 62 (2016) 988–1011. doi:10.1016/j.rser.2016.05.045.

[3] B. P. Jelle, Traditional, state-of-the-art and future thermal building insulation materials and solutions - Properties, requirements and possibilities, Energy and Buildings 43 (10) (2011) 2549–2563. doi:10.1016/j.enbuild.2011.05.015.

[4] F. Asdrubali, A. L. Pisello, F. D'Alessandro, F. Bianchi, C. Fabiani, M. Cornicchia, A. Rotili, Experimental and numerical characterization of innovative cardboard based panels: Thermal and acoustic performance analysis and life cycle assessment, Building and Environment 95 (2016) 145–159. doi:10.1016/j.buildenv.2015.09.003.

[5] L. Aditya, T. M. Mahlia, B. Rismanchi, H. M. Ng, M. H. Hasan, H. S. Metselaar, O. Muraza, H. B. Aditiya, A review on insulation materials for energy conservation in buildings, Renewable and Sustainable Energy Reviews 73 (2017) 1352–1365. doi:10.1016/j.rser.2017.02.034.

[6] L. C. O. Souza, H. A. Souza, E. F. Rodrigues, Experimental and numerical analysis of a naturally ventilated double-skin façade, Energy and Buildings 165 (2018) 328–339. doi:10.1016/J.ENBUILD.2018.01.048.

[7] W. Ding, Y. Hasemi, T. Yamada, Natural ventilation performance of a double-skin façade with a solar chimney, Energy and Buildings 37 (4) (2005) 411–418. doi:10.1016/j.enbuild.2004.08.002.

[8] L. Gullbrekken, T. Kvande, Ventilated wooden roofs: Influence of local weather conditions - measurements, Energy Procedia 132 (2017) 777–782. doi:10.1016/J.EGYPRO.2017.10.029.

[9] R. Seblany, N. Ghaddar, K. Ghali, N. Ismail, M. Simonetti, J. Virgone, A. Zoughaib, Humidity control of liquid desiccant membrane ceiling and displacement ventilation system, Applied Thermal Engineering 144 (2018) 1–12. doi:10.1016/j.applthermaleng.2018.08.036.

[10] H. Lim, Y.-K. Kang, J.-W. Jeong, Thermoelectric radiant cooling panel design: Numerical simulation and experimental validation, Applied Thermal Engineering 144 (2018) 248–261. doi:10.1016/j.applthermaleng.2018.08.065.

[11] C. Yadav, R. R. Sahoo, Exergy and energy comparison of organic phase change materials based thermal energy storage system integrated with engine exhaust, Journal of Energy Storage 24 (2019) 100773. doi:10.1016/J.EST.2019.100773.

[12] F. Souayfane, F. Fardoun, P. H. Biwole, Phase change materials (PCM) for cooling applications in buildings: A review, Energy and Buildings 129 (2016) 396–431. doi:10.1016/j.enbuild.2016.04.006.

[13] K. A. Aly, A. R. El-Lathy, M. A. Fouad, Enhancement of solidification rate of latent heat thermal energy storage using corrugated fins, Journal of Energy Storage 24. doi:10.1016/j.est.2019.100785.

[14] F. Bruno, M. Belusko, M. Liu, N. H. S. Tay, 9 - Using solid-liquid phase change materials (PCMs) in thermal energy storage systems, in: L. F. Cabeza (Ed.), Advances in Thermal Energy Storage Systems, Woodhead Publishing Series in Energy, Woodhead Publishing, 2015, pp. 201–246. doi:https://doi.org/10.1533/9781782420965.2.201.

[15] A. D'Alessandro, C. Fabiani, A. L. Pisello, F. Ubertini, A. L. Materazzi, F. Cotana, Innovative concretes for low-carbon constructions: a review, International Journal of Low-Carbon Technologies 12 (3) (2016) 289–309. doi:10.1093/ijlct/ctw013.

[16] A. Sar, A. Bicer, A. Al-Ahmed, F. A. Al-Sulaiman, M. H. Zahir, S. A. Mohamed, Silica fume/capric acid-palmitic acid composite phase change material doped with CNTs for thermal energy storage, Solar Energy Materials and Solar Cells 179 (2018) 353–361. doi:10.1016/J.SOLMAT.2017.12.036.

[17] S. Kahwaji, M. B. Johnson, A. C. Kheirabadi, D. Groulx, M. A. White, Fatty acids and related phase change materials for reliable thermal energy storage at moderate temperatures, Solar Energy Materials and Solar Cells 167 (2017) 109–120. doi:10.1016/j.solmat.2017.03.038.

[18] Y. Lin, C. Zhu, G. Alva, G. Fang, Palmitic acid/polyvinyl butyral/expanded graphite composites as form-stable phase change materials for solar thermal energy storage, Applied Energy 228 (2018) 1801–1809. doi:10.1016/J.APENERGY.2018.07.068.

[19] J. A. Noël, P. M. Allred, M. A. White, Life cycle assessment of two biologically produced phase change materials and their related products, The International Journal of Life Cycle Assessment 20 (3) (2015) 367–376. doi:10.1007/s11367-014-0831-1.

[20] V. Brancato, A. Frazzica, A. Sapienza, A. Freni, Identification and characterization of promising phase change materials for solar cooling applications, Solar Energy Materials and Solar Cells 160 (2017) 225–232. doi:10.1016/j.solmat.2016.10.026.

[21] A. de Gracia, L. Navarro, A. Castell, Á. Ruiz-Pardo, S. Alvárez, L. F. Cabeza, Experimental study of a ventilated facade with PCM during winter period, Energy and Buildings 58 (2013) 324–332. doi:10.1016/J.ENBUILD.2012.10.026.

[22] L. Shilei, Z. Neng, F. Guohui, Impact of phase change wall room on indoor thermal environment in winter, Energy and Buildings 38 (1) (2006) 18–24. doi:10.1016/J.ENBUILD.2005.02.007.

[23] Y. Konuklu, H. Paksoy, Phase change material sandwich panels for managing solar gain in buildings, Journal of Solar Energy Engineering, Transactions of the ASME 131 (4) (2009) 0410121–0410127. doi:10.1115/1.3197839.

[24] A. D'Alessandro, A. L. Pisello, C. Fabiani, F. Ubertini, L. F. Cabeza, F. Cotana, Multifunctional smart concretes with novel phase change materials: Mechanical and thermo-energy investigation, Applied Energy 212 (2018) 1448–1461. doi:10.1016/J.APENERGY.2018.01.014.

[25] L. Desgrosseilliers, C. A. Whitman, D. Groulx, M. A. White, Dodecanoic acid as a promising phase-change material for thermal energy storage, Applied Thermal Engineering 53 (1) (2013) 37–41. doi:10.1016/j.applthermaleng.2012.12.031.

[26] Y. Yanping, Z. Nan, T. Wenquan, C. Xiaoling, H. Yaling, Fatty acids as phase change materials: A review, Renewable and Sustainable Energy Reviews 29 (2014) 482–498. doi:10.1016/j.rser.2013.08.107.

[27] M. C. Floros, S. S. Narine, Saturated linear diesters from stearic acid as renewable phase change materials, Materials Letters 137 (2014) 252–255. doi:10.1016/J.MATLET.2014.09.041.

[28] M. C. Floros, S. S. Narine, Latent heat storage using renewable saturated diesters as phase change materials, Energy 115 (2016) 924–930. doi:10.1016/J.ENERGY.2016.09.085.

[29] R. Latchmi, Y. Jin, N. S. S., Synthesis and Characterization of Novel Diol, Diacid and Diisocyanate from Oleic Acid, Journal of the American Oil Chemists' Society 91 (2) 349–356. doi:10.1007/s11746-013-2376-z.

[30] D. Feldman, D. Banu, D. Hawes, Low chain esters of stearic acid as phase change materials for thermal energy storage in buildings, Solar Energy Materials and Solar Cells 36 (3) (1995) 311–322. doi:10.1016/0927-0248(94)00186-3.

[31] M. Alomair, Y. Alomair, S. Tasnim, S. Mahmud, H. Abdullah, Analyses of Bio-Based Nano-PCM filled Concentric Cylindrical Energy Storage System in Vertical Orientation, Journal of Energy Storage 20 (2018) 380–394. doi:10.1016/j.est.2018.10.004.

[32] L. Raghunanan, M. C. Floros, S. S. Narine, Thermal stability of renewable diesters as phase change materials, Thermochimica Acta 644 (2016) 61–68. doi:10.1016/j.tca.2016.10.009.

[33] R. Nikolić, M. Marinović-Cincović, S. Gadžurić, I. Zsigrai, New materials for solar thermal storagesolid/liquid transitions in fatty acid esters, Solar Energy Materials and Solar Cells 79 (3) (2003) 285–292. doi:10.1016/S0927-0248(02)00412-9.

[34] R. K. Sharma, P. Ganesan, V. V. Tyagi, H. S. Metselaar, S. C. Sandaran, Developments in organic solid-liquid phase change materials and their applications in thermal energy storage, Energy Conversion and Management 95 (2015) 193–228. doi:10.1016/j.enconman.2015.01.084.

[35] S. Wi, J. Seo, S. G. Jeong, S. J. Chang, Y. Kang, S. Kim, Thermal properties of shape-stabilized phase change materials using fatty acid ester and exfoliated graphite nanoplatelets for saving energy in buildings, Solar Energy Materials and Solar Cells 143 (2015) 168–173. doi:10.1016/j.solmat.2015.06.040.

[36] A. Mancini, E. Imperlini, E. Nigro, C. Montagnese, A. Daniele, S. Orrù, P. Buono, Biological and nutritional properties of palm oil and palmitic acid: Effects on health, Molecules 20 (9) (2015) 17339–17361. doi:10.3390/molecules200917339.

[37] K. Chetehouna, N. Belayachi, B. Rengel, D. Hoxha, P. Gillard, Investigation on the thermal degradation and kinetic parameters of innovative insulation materials using TGA-MS, Applied Thermal Engineering 81 (2015) 177–184. doi:10.1016/J.APPLTHERMALENG.2015.02.037.

[38] E. K. Asimakopoulou, D. I. Kolaitis, M. A. Founti, Fire safety aspects of PCM-enhanced gypsum plasterboards: An experimental and numerical investigation, Fire Safety Journal 72 (2015) 50–58. doi:10.1016/J.FIRESAF.2015.02.004.

[39] S. Vyazovkin, A. K. Burnham, J. M. Criado, L. A. Pérez-Maqueda, C. Popescu, N. Sbirrazzuoli, ICTAC Kinetics Committee recommendations for performing kinetic computations on thermal analysis data, Thermochimica Acta 520 (1-2) (2011) 1–19. doi:10.1016/J.TCA.2011.03.034.

[40] C. Buratti, S. Mousavi, M. Barbanera, E. Lascaro, F. Cotana, M. Bufacchi, Thermal behaviour and kinetic study of the olive oil production chain residues and their mixtures during co-combustion, Bioresource Technology 214 (2016) 266–275. doi:10.1016/j.biortech.2016.04.097.

[41] F. Carrasco, P. Pagès, J. Gámez-Pérez, O. Santana, M. Maspoch, Kinetics of the thermal decomposition of processed poly(lactic acid), Polymer Degradation and Stability 95 (12) (2010) 2508–2514. doi:10.1016/J.POLYMDEGRADSTAB.2010.07.039.

[42] M. Starink, The determination of activation energy from linear heating rate experiments: a comparison of the accuracy of isoconversion methods, Thermochimica Acta 404 (1-2) (2003) 163–176. doi:10.1016/S0040-6031(03)00144-8.

[43] K. Miura, T. Maki, A Simple Method for Estimating f (E) and k <sub>0</sub> ( E ) in the Distributed Activation Energy Model, Energy & Fuels 12 (5) (1998) 864–869. doi:10.1021/ef970212q.

[44] D. C. D., Estimating isothermal life from thermogravimetric data, Journal of Applied Polymer Science 6 (24) 639–642. doi:10.1002/app.1962.070062406.

[45] Kinetic study of a thermal dechlorination and oxidation of neodymium oxychloride, Thermochimica Acta 460 (1-2) (2007) 53–59. doi:10.1016/J.TCA.2007.05.019.

[46] International Organization for Standardization, ISO 14040: Environmental management - Life cycle assessment - Principles and framework, Tech. Rep. 1 (2006). doi:10.1136/bmj.332.7550.1107.

[47] International Organization for Standardization, ISO 14044: Environmental management - Life cycle assessment - Requirements and guidelines, Tech. Rep. 571 (2007). doi:10.1007/s11367-011-0297-3.

[48] T. I. E. S. EPD, Product Category Rules (PCR): Construction Products and Construction Services - 2012:01 - Version 2.3, Tech. rep. (2018).

[49] Rubitherm, RT4 Data sheet, Tech. rep. (2009).

[50] Rubitherm, RT31 Data Sheet, Tech. rep. (2009).

[51] R. Hischier, B. Weidema, H.-J. Althaus, C. Bauer, G. Doka, R. Dones, R. Frischknecht, S. Hellweg, S. Humbert, N. Jungbluth, T. Köllner, Y. Loerincik, M. Margni, T. Nemecek, Implementation of Life Cycle Impact Assessment Methods. ecoinvent report No. 3, v2.2 Swiss Centre for Life Cycle Inventories, Dübendorf, Ecoinvent (3).

[52] J. Li, J. Liu, X. Sun, Y. Liu, The mathematical prediction model for the oxidative stability of vegetable oils by the main fatty acids composition and thermogravimetric analysis, LWT 96 (2018) 51–57. doi:10.1016/J.LWT.2018.05.003.

[53] E. S. Kenda, K. E. N'Tsoukpoe, I. W. Ouédraogo, Y. Coulibaly, X. Py, F. M. A. W. Ouédraogo, Jatropha curcas crude oil as heat transfer fluid or thermal energy storage material for concentrating solar power plants, Energy for Sustainable Development 40 (2017) 59–67. doi:10.1016/J.ESD.2017.07.003.

[54] D. Trache, F. Maggi, I. Palmucci, L. T. DeLuca, Thermal behavior and decomposition kinetics of composite solid propellants in the presence of amide burning rate suppressants, Journal of Thermal Analysis and Calorimetry 132 (3) (2018) 1601–1615. doi:10.1007/s10973-018-7160-8.

[55] Y.-g. Liang, B. Cheng, Y.-b. Si, D.-j. Cao, H.-y. Jiang, G.-m. Han, X.-h. Liu, Thermal decomposition kinetics and characteristics of Spartina alterniflora via thermogravimetric analysis, Renewable Energy 68 (2014) 111–117. doi:10.1016/J.RENENE.2014.01.041.

[56] H. Li, S. Niu, C. Lu, Y. Wang, Comprehensive Investigation of the Thermal Degradation Characteristics of Biodiesel and Its Feedstock Oil through TGA-FTIR, Energy and Fuels 29 (8) (2015) 5145–5153. doi:10.1021/acs.energyfuels.5b01054.

[57] V. Volli, M. Purkait, Physico-chemical properties and thermal degradation studies of commercial oils in nitrogen atmosphere, Fuel 117 (2014) 1010–1019. doi:10.1016/J.FUEL.2013.10.021.

[58] A. S. Reshad, P. Tiwari, V. V. Goud, Thermal Degradation Kinetic Study of Rubber Seed Oil and Its Methyl Esters under Inert Atmosphere, Energy & Fuels 31 (9) (2017) 9642–9651. doi:10.1021/acs.energyfuels.7b02249.

[59] R. M. Mahfouz, M. A. S. Monshi, A. Al-Owais, S. Alshehri, M. M. Al-Osaimi, N. M. A. El-Salam, $\gamma$-irradiation effects on kinetics and mechanism of the thermal decomposition of zinc acetate, Radiation Effects and Defects in Solids 159 (1) (2004) 7–15. doi:10.1080/10420150310001618223.

[60] S. C. Turmanova, S. D. Genieva, A. S. Dimitrova, L. T. Vlaev, Non-isothermal degradation kinetics of filled with rise husk ash polypropene composites, Express Polymer Letters 2 (2) (2008) 133–146. doi:10.3144/expresspolymlett.2008.18.

[61] Y. C. Man, K. Shamsi, M. Yusoff, S. Jinap, A study on the crystal structure of palm oil-based whipping cream, Journal of the American Oil Chemists' Society 80 (5) (2003) 409–415. doi:10.1007/s11746-003-0713-1.

[62] C. L. Chong, Z. Kamarudin, P. Lesieur, A. Marangoni, C. Bourgaux, M. Ollivon, Thermal and structural behaviour of crude palm oil: crystallisation at very slow cooling rate, European journal of lipid science and technology 109 (4) (2007) 410–421. doi:10.1002/ejlt.200600249.

[63] A. Watanabe, I. Tashima, N. Matsuzaki, J. Kurashige, K. Sato, On the formation of granular crystals in fat blends containing palm oil, Journal of the American Oil Chemists' Society 69 (11) (1992) 1077–1080. doi:10.1007/BF02541040.

[64] M. Goedkoop, R. Heijungs, M. Huijbregts, A. D. Schryver, J. Struijs, R. V. Zelm, ReCiPe 2008, A life cycle impact assessment method which comprises harmonised category indicators at the midpoint and the endpoint level, Tech. Rep. May 2016 (2008). doi:10.029/2003JD004283.

Table 4: Most frequently mechanism functions and their integral forms using in TGA kinetic with the sum of the standard deviations between the theoretical master and the experimental data.

| Mechanism | Symbol | f($\alpha$) | g($\alpha$)[a] | $\Sigma\delta$ |
|---|---|---|---|---|
| *Order of reaction* | | | | |
| First-order | $FF_1$ | 1-$\alpha$ | -ln(1-$\alpha$) | 0.462 |
| Second-order | $FF_2$ | $(1\text{-}\alpha)^2$ | $(1\text{-}\alpha)^{-1}$-1 | 2.388 |
| Third-order | $FF_3$ | $(1\text{-}\alpha)^3$ | $\left[(1-\alpha)^{-2}-1\right]/2$ | 9.844 |
| *Diffusion* | | | | |
| One-way transport | $DD_1$ | $0.5\alpha$ | $\alpha^2$ | 0.554 |
| Two-way transport | $DD_2$ | $\left[-\ln(1-\alpha)\right]^{-1}$ | $(1-\alpha)\ln(1-\alpha)+\alpha$ | 0.990 |
| Three-way transport | $DD_3$ | $1.5(1-\alpha)^{2/3}\left[1-(1-\alpha)^{1/3}\right]^{-1}$ | $\left[1-(1-\alpha)^{1/3}\right]^2$ | 1.850 |
| Ginstling-Brounshtein equation | $DD_4$ | $1.5\left[(1-\alpha)^{-1/3}-1\right]^{-1}$ | $(1-2\alpha/3)-(1-\alpha)^{2/3}$ | 1.234 |
| *Limiting surface reaction between both phases* | | | | |
| One dimension | $RR_1$ | 1 | $\alpha$ | 0.183 |
| Two dimensions | $RR_2$ | $2(1-\alpha)^{1/2}$ | 1-$(1-\alpha)^{1/2}$ | 0.123 |
| Three dimensions | $RR_3$ | $3(1-\alpha)^{2/3}$ | 1-$(1-\alpha)^{1/3}$ | 0.202 |
| *Random nucleation and nuclei growth* | | | | |
| Two-dimensional | $AA_2$ | $2(1-\alpha)\left[-\ln(1-\alpha)\right]^{1/2}$ | $\left[-\ln(1-\alpha)\right]^{1/2}$ | 0.249 |
| Three-dimensional | $AA_3$ | $3(1-\alpha)\left[-\ln(1-\alpha)\right]^{2/3}$ | $\left[-\ln(1-\alpha)\right]^{1/3}$ | 0.406 |
| *Exponential nucleation* | | | | |
| Power law, n=1/2 | $PP_2$ | $2\alpha^{1/2}$ | $\alpha^{1/2}$ | 0.433 |
| Power law, n=1/3 | $PP_3$ | $3\alpha^{2/3}$ | $\alpha^{1/3}$ | 0.521 |
| Power law, n=1/4 | $PP_4$ | $4\alpha^{3/4}$ | $\alpha^{1/4}$ | 0.568 |

[a] g($\alpha$) is the integral form of f($\alpha$)

Table 5: Pre-exponential factor calculated for different heating rates.

| Heating rate ($K \cdot min^{-1}$) | A ($s^{-1}$) | $R^2$ |
|---|---|---|
| 5 | 2.27E+08 | 0.9859 |
| 7 | 2.51E+08 | 0.9743 |
| 10 | 2.71E+08 | 0.9990 |
| 15 | 3.15E+08 | 0.9989 |
| Average | 26.6E+07 | |
| Standard deviation | 3.7E+07 | |

Table 6: Thermophysical characterisation of the studied bio-based PCM (p1 = first melting peak, p2 = second melting peak).

| Aging cycles | Number of peak [K] | Onset melting temperature [K] | Melting peak [K] | Latent heat of fusion [$kJ \cdot kg^{-1}$] | Percentage variation [%] |
|---|---|---|---|---|---|
| 0 | p1 | 264.4 | 276.4 | 33 | – |
| | p2 | 297.2 | 307.0 | 14 | – |
| 100 | p1 | 264.2 | 276.7 | 32 | 3.0 |
| | p2 | 299.0 | 308.7 | 13 | 1.8 |
| 1000 | p1 | 264.2 | 278.9 | 30 | 9.1 |
| | p2 | 299.5 | 309.1 | 13 | 1.8 |
| 10000 | p1 | 264.0 | 279.3 | 26 | 21.4 |
| | p2 | 300.5 | 310.0 | 13 | 5.6 |

Table 7: Maximum (M) and inflection points ($I_{1--9}n$) of the three average temperature trends at H1 = 1 cm, H2 = 3.5 cm and H3 = 6 cm.

| | H1 | | H2 | | H3 | |
|---|---|---|---|---|---|---|
| | t (hh:mm:ss) | T (K) | t (hh:mm:ss) | T (K) | t (hh:mm:ss) | T (K) |
| $I_1$ | 03:59:26 | 274.7 | 03:57:49 | 274.9 | 03:06:35 | 273.9 |
| $I_2$ | 05:41:51 | 279.2 | 05:39:50 | 279.4 | 04:44:06 | 279.3 |
| $I_3$ | 11:39:06 | 301.4 | 11:30:52 | 301.0 | 10:54:09 | 303.3 |
| $I_4$ | 13:42:58 | 311.8 | 13:26:21 | 310.6 | 13:20:27 | 314.0 |
| $I_5$ | 30:09:53 | 306.9 | 30:11:07 | 307.1 | 30:01:01 | 307.8 |
| $I_6$ | 32:16:05 | 300.8 | 32:16:28 | 301.1 | 32:07:53 | 300.2 |
| $I_7$ | 34:26:52 | 294.3 | 34:26:49 | 294.6 | 34:20:37 | 292.0 |
| $I_8$ | 36:25:39 | 286.2 | 36:25:01 | 286.4 | 36:33:42 | 283.0 |
| $I_9$ | 39:17:46 | 277.1 | 39:14:58 | 277.5 | 37:28:59 | 279.7 |
| M | 23:07:51 | 333.5 | 23:08:14 | 333.5 | 22:58:56 | 333.5 |